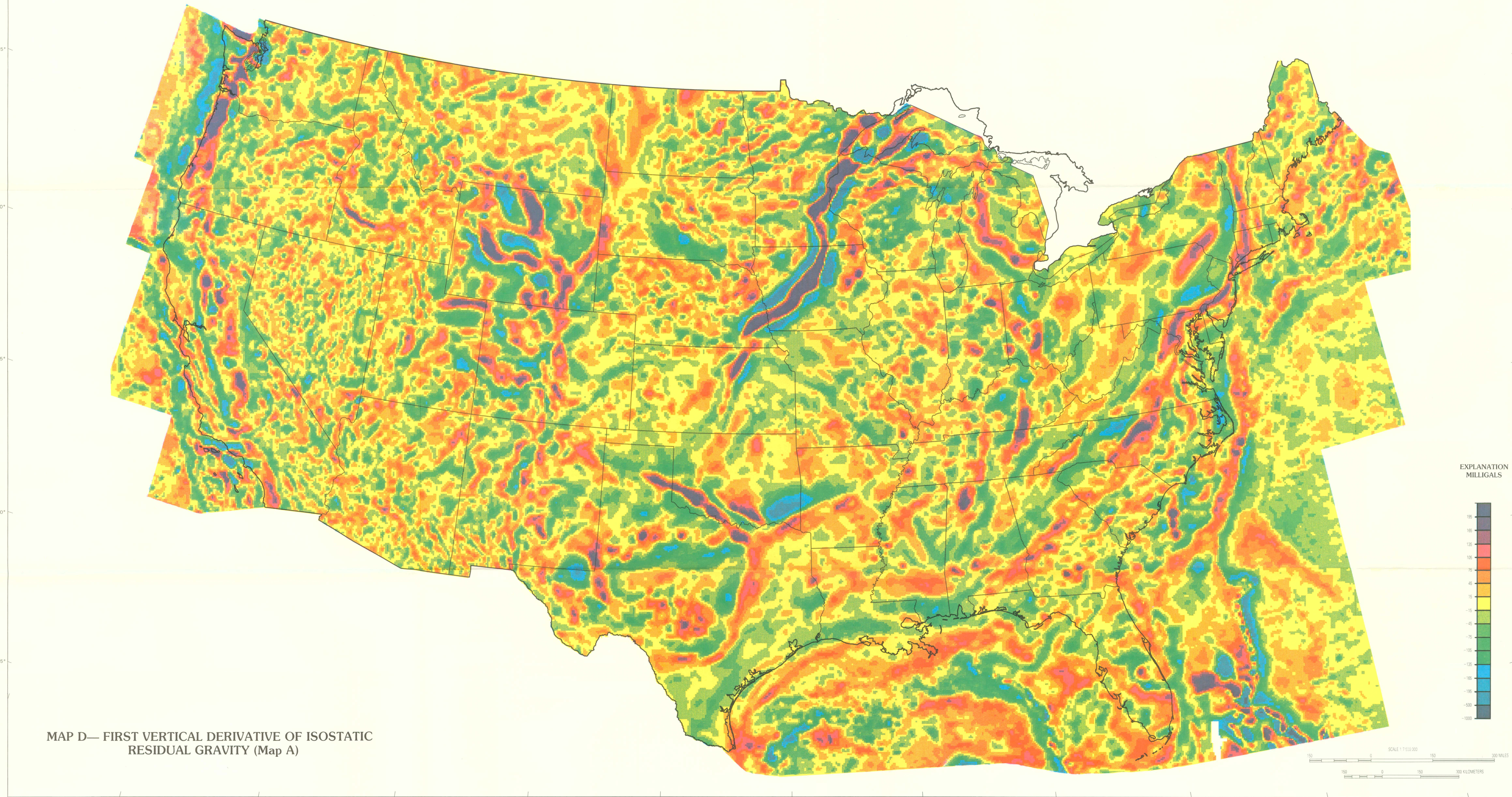


MAP C—ISOSTATIC RESIDUAL GRAVITY

Isostatic correction based on Airy-Heiskanen local compensation model with parameters: 2.67 g/cm³ for density of topographic load, 21.7 km for depth to bottom of root under sea-level elevations, and 0.885 g/cm³ for density contrast across bottom of root. Certain offshore anomalies with widths less than about 40 km may be in error by 40 mGal or more—they are artifacts of the Bouguer correction that was applied to the offshore free-air gravity data (see text), and they appear as small spikes of color in areas where bottom depths are changing rapidly.

Gravity data obtained from Society of Exploration Geophysicists (1982) and Cohen and Scholer (1982).



MAP D—FIRST VERTICAL DERIVATIVE OF ISOSTATIC RESIDUAL GRAVITY (Map A)

Larger wavelength anomalies do not provide much information about isostatic equilibrium either. Many long-wavelength anomalies are probably caused by sources in the mantle below the depth of compensation and below the isostatic system. Other long-wavelength anomalies can be modeled by geologically reasonable density contrasts confined to the crust and upper mantle and assumed to be in complete isostatic equilibrium.

Gravity data obtained from Society of Exploration Geophysicists (1982) and Cohen and Scholer (1982).

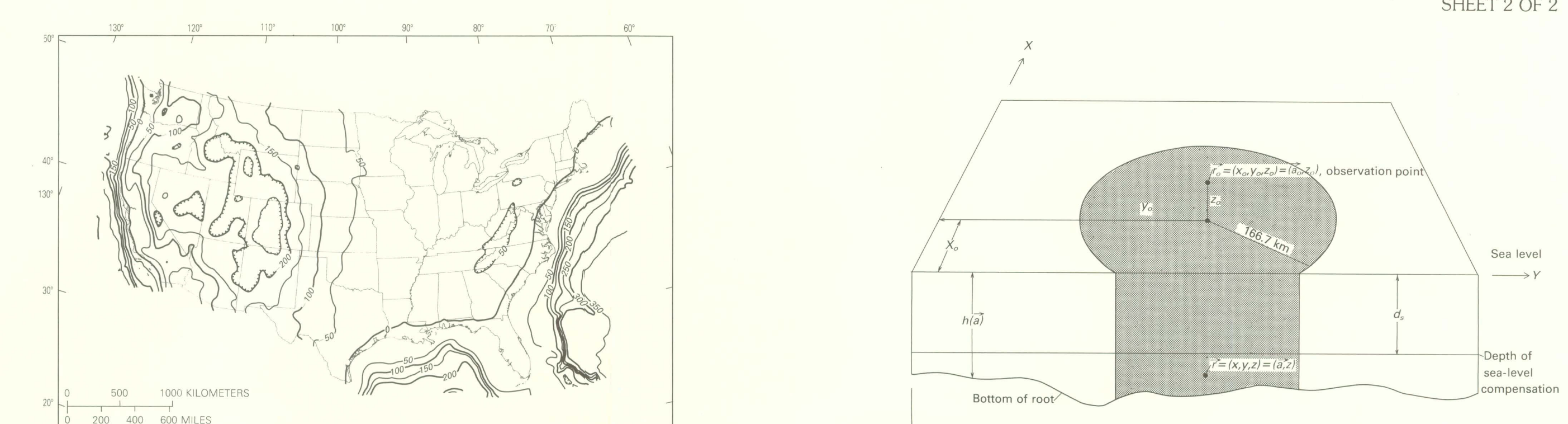


Figure 6—Isostatic regional gravity field in mGal at sea level. This is the gravitational attraction of the compensating masses (roots) in the Airy-Heiskanen model with same parameters as in Figure 5. This attraction is subtracted from the Bouguer gravity field as an isostatic correction to give the isostatic residual gravity (map A). Buckles on closed contours point toward low regional values.

Text continued from sheet 1 of 2.

COMPARISON OF THE ISOSTATIC RESIDUAL MAPS

Visual comparison of the two isostatic residual maps (maps A and C) reveals only slight changes in the offshore anomaly values. The most apparent change is a shift of about 10 mGal in the colors of the low anomaly in the Atlantic Ocean offshore from North Carolina. As discussed in the calculation section, we believe that this change is in large part caused by the mismatch of our parameters for the calculation out to 166.7 km with the parameters used in the published edition of Kirtzi and others (1981) for the area beyond 7 km. We expect that map C is a more accurate representation because the largest mismatch is no more than about 1 mGal offshore.

Additional comparison tests are summarized in table 2. They compare on-land isostatic corrections (inside a 166.7 km radius) for the conterminous United States for different choices of parameters in the Airy-Heiskanen compensation model. The parameters chosen probably cover the range of reasonable choices for the Airy-Heiskanen model applied to the conterminous United States. It is apparent that changing model parameters over a considerable range of values should not significantly alter the appearance of isostatic residual maps.

For the enhancement and interpretation of anomalies caused by shallow geologic features, the application of some isostatic residual maps is more important than the exact details of the model used. This point is well made by comparing the two isostatic residual maps (maps A and C) with a Bouguer gravity map of the same area.

CAUTION ON THE SIGNIFICANCE OF ISOSTATIC ANOMALIES

There is a common tendency to attribute anomalies on an isostatic residual map to isostatic imbalance—that is, to loads which are not properly compensated. In this view, anomalous high might imply undercompensation and consequent tectonic subsidence, whereas low might indicate overcompensation and consequent uplift.

Most anomalies with widths less than several hundred kilometers—especially equidimensional anomalies as opposed to elongated two-dimensional ones—can be explained equally well in terms of density inhomogeneities in the crust that are perfectly compensated at depths less than 50 km. This point is best made by reference to a simple example. A mountain resting on a uniform crust (Fig. 7) is supported by a local Airy-Heiskanen root. On an isostatic residual map no anomaly would appear, because the effect of the mountain is removed by the Bouguer correction and the effect of its root is removed by the isostatic correction. In Figure 8, a dense mass in the upper crust is also supported by a local root. Because there is no topography in this case, neither the effect of the mass nor of its compensation has been removed. The compensating root produces a gravity anomaly that is broader and of lower amplitude than that produced by the mass. For the example in figure 8, the net result is a substantial anomaly even though the mass is completely compensated. In principle, the presence of compensating masses could be inferred from the characteristics of the total anomaly—a residual anomaly of one sign flanked by broader anomalies of the opposite sign and a total anomaly that integrates to zero. In practice, however, the flanking anomalies frequently are masked by neighboring anomalies and cannot be clearly distinguished.

CONCLUSIONS

1. Isostatic residual gravity maps of continental areas are easy to make and comparisons with one the gravity data and topographic data are available in digital form. Editing and correcting these digital data sets remains the most difficult part of the job.
2. For purposes of displaying anomalies, trends, and patterns caused by features of geologic interest, the choice of isostatic model is less important than the application of an isostatic correction of some sort. Most reasonable compensation models will produce an isostatic residual that approximates the effect of upward continuing the topography as if it were a potential field to some height related to the depth of compensation. (A constant multiplier must also be applied to convert elevations to mGal.) The two isostatic residual gravity maps (maps A and C) illustrate the relatively minor difference in map patterns produced by various isostatic models. These differences are of less interest than the overall patterns if the goal is to highlight shallow density contrasts of geologic importance.
3. It is almost impossible to determine from the gravity data alone whether individual isostatic residual anomalies imply local isostatic balance or imbalance. Probably the most productive approach for interpreting such anomalies is to assume that they are completely compensated and to use as much geologic and geophysical data as construct a density model of the source bodies. If the bodies are not in isostatic balance, then this should become apparent in the modeling process if enough additional geologic and geophysical constraints are available.

ACKNOWLEDGMENTS

We would like to thank James Case, Andrew Groom, Carl Westworth, and Mark Zoback for their long-standing encouragement and interest in the preparation of this map. The results have been much improved by their comments and by the criticism of Warren Hamilton, David Harwood, Walter Moore, David Poole, Ray Wells, and Mary Lou Zoback. Many others have also freely shared their ideas and insights into the meanings of the isostatic anomalies and we are most grateful for the stimulus that they have provided.

APPENDIX

ATTRACTION OF AIRY-HEISKANEN ROOT TO 166.7 KM

This appendix contains a derivation of the equations used to calculate the vertical attraction of an Airy-Heiskanen isostatic root out to a distance of 166.7 km from the observation point. The method is a modification of the technique proposed by Parker (1972) for the rapid calculation of potential anomaly and part of the derivation is identical to that given by Parker. The geometry used is shown in figure 9.

The Parker algorithm allows the calculation of the attraction of a root on a flat Earth out to "infinity" (that is, to the limits of the data grid) in the x and y directions. We chose to calculate the attraction of the root only out to 166.7 km from an observation point, and to express this contribution with published results for the portion of the Earth's surface from 166.7 km to the antipode. This is accomplished by first computing the integral to "infinity" by Parker's algorithm, and then subtracting another integral from 166.7 km to "infinity". Because of the geometry, this second integral is usually small compared to the first (12 percent for a flat root at 40 km). Evaluation of the second integral involves the numerical integration of an integral containing a Bessel function, as will be seen below. This approach, although seemingly rather complicated, saves considerable time in computation over a more direct method that calculates and sums the attraction of individual mass elements out to 166.7 km (Jachens and Roberts, 1981).

For topography above sea level, the corresponding root extends from a depth d_0 of compensation for sea level to a depth d_1 determined by the Airy-Heiskanen equations. For areas covered by ocean, the antipode rise above sea level h is convenient to substitute the attraction of a root extending from sea level ($x=0$) down to the appropriate depth d_1 , and as a last step to subtract the attraction of a flat-bottomed cylinder between 0 and d_0 .

The definition of the two-dimensional Fourier transform and its inverse used in this derivation is

$$F(f) = \int_{-\infty}^{\infty} f(x) e^{-ifx} dx \quad (1)$$

$$f(x) = \frac{1}{2\pi} \int_{-\infty}^{\infty} F(f) e^{ifx} df \quad (2)$$

where $\vec{x} = (x, y)$ is a two-dimensional vector lying in a horizontal plane, and $\vec{f} = (f_x, f_y)$ is the corresponding wave-number vector. A general position vector $\vec{r} = (r, \theta)$ can be represented also as $\vec{r} = (r, \phi)$. The point at which gravity is observed is indicated by the subscript zero as in $\vec{r}_0 = (r_0, \theta_0)$. Note that in the derivation here, x increases downward.

$$s_x(\vec{r}) = - \iint G_0 \frac{\partial}{\partial x} \left(\frac{\rho_0 - \rho_1}{r} \right) dV \quad (3)$$

where V is the volume between $x=0$ and $x=R$ within a radius $R=166.7$ km observation point \vec{r}_0 . This can be rewritten as

$$s_x(\vec{r}) = -G_0 \int_0^R \int_0^{2\pi} \int_0^{2\pi} \frac{\partial}{\partial x} \left(\frac{\rho_0 - \rho_1}{r} \right) r dr d\theta d\phi \quad (4)$$

where $\vec{r} = (r, \theta)$ is a two-dimensional vector lying in a horizontal plane, and $\vec{f} = (f_x, f_y)$ is the corresponding wave-number vector. A general position vector $\vec{r} = (r, \theta)$ can be represented also as $\vec{r} = (r, \phi)$. The point at which gravity is observed is indicated by the subscript zero as in $\vec{r}_0 = (r_0, \theta_0)$. Note that in the derivation here, x increases downward.

$$s_x(\vec{r}) = -G_0 \int_0^R \int_0^{2\pi} \int_0^{2\pi} \frac{\partial}{\partial x} \left(\frac{\rho_0 - \rho_1}{r} \right) r dr d\theta d\phi \quad (5)$$

Changing variables within the inner double integral by using $\vec{r} = \vec{r}_0 + \vec{r}'$ and $\vec{f} = \vec{f}_0 + \vec{f}'$, converting the double integral to polar coordinates, and using the relation $\int_0^{2\pi} e^{-if'_x r'} d\theta' = 2\pi J_0(f'_x r')$

$$s_x(\vec{r}) = -G_0 \int_0^R \int_0^{2\pi} \frac{\partial}{\partial x} \left(\frac{\rho_0 - \rho_1}{r} \right) r dr d\theta \quad (6)$$

From Braccioni (1965, p. 247), we get

$$s_x(\vec{r}) = -G_0 \int_0^R \int_0^{2\pi} \frac{\partial}{\partial x} \left(\frac{\rho_0 - \rho_1}{r} \right) r dr d\theta \quad (7)$$

More details of this part of the derivation given by Parker (1972) and Blakely (1981).

The second integral I_2 from $R=166.7$ km to ∞ can be evaluated with the help of a series expansion:

$$\left(\frac{a^2 + x^2}{a^2} \right)^{-3/2} = a^{-2} \left(1 - \frac{3x^2}{2a^2} + \frac{15x^4}{8a^4} - \dots \right) \quad (8)$$

When this expansion is substituted into equation (8), the x integration can be performed yielding

$$s_x(\vec{r}) = -2\pi G_0 \int_0^R \int_0^{2\pi} \frac{\partial}{\partial x} \left(\frac{\rho_0 - \rho_1}{r} \right) r dr d\theta \quad (9)$$

which can be recognized to give

$$s_x(\vec{r}) = -2\pi G_0 \int_0^R \int_0^{2\pi} F(f) e^{-ifx} df \quad (10)$$

The integral I_2 can be simplified slightly for numerical integration to

$$s_x(\vec{r}) = -2\pi G_0 \int_0^R \int_0^{2\pi} F(f) e^{-ifx} df \quad (11)$$

For root depths small compared to 166.7 km, the series in (10) converges rapidly. For example, for $x=40$ the second term is approximately 4 percent of the first, and since the attraction beyond 166.7 km is probably less than 25 percent of the whole in most cases (Woodward, 1966), using only the first term in the expansion would result in an error for a flat root with sea base 40 km of approximately 1 percent (1 to 2 mGal). Thus, convergence is expected to be rapid for all but the most extreme cases.

ISOSTATIC RESIDUAL GRAVITY, TOPOGRAPHIC, AND FIRST-VERTICAL-DERIVATIVE GRAVITY MAPS OF THE CONTERMINOUS UNITED STATES

By
R.W. Simpson, R.C. Jachens, R.W. Saltus, and R.J. Blakely
1986